Title: Mindfulness meditation changes the boundary and configuration of the primary functional networks in the brain.

Authors: Shogo Kajimura[1,2,*], Naoki Masuda[3], Johnny King Lau[4], Kou Murayama[4]

[1]Faculty of Information and Human Science, Kyoto Institute of Technology, Kyoto, Japan; [2]Department of Psychology, University of York, York, UK; [3]Department of Engineering Mathematics, University of Bristol, UK; [4]Department of Psychology, University of Reading, UK

***Corresponding author**:

Faculty of Information and Human Science, Kyoto Institute of Technology, Kyoto, Japan

1, Matsugasakihashigami-cho, Sakyo-ku, Kyoto-shi, Kyoto, 606-8585, Japan

E-mail address: kajimura.shogo.1204@gmail.com

Keywords: mindfulness practice; community structure; complex network; intervention; single-case design

Abstract

Research has shown that mindfulness meditation not only improves our cognitive and motivational functioning (e.g., attention, mental health), it influences the way how our brain networks [e.g., default mode network (DMN), front-parietal network (FPN), and sensory-motor network (SMN)] function and operate. However, surprisingly little attention has been paid to the possibility that mindfulness meditation alters the structure (composition) of these functional brain networks. Here, using a single-case experimental design with longitudinal intensive data, we examined the effect of mindfulness mediation on intra-individual changes in the composition of whole-brain networks. The results showed that mindfulness meditation (1) changed the community size (with a number of regions in the FPN being merged into the DMN after mindfulness meditation), (2) changed the brain regions composing the SMN community without changing its size, and (3) led to instability in the community allegiance of the regions in the FPN. These results suggest that, in addition to altering specific functional connectivity, mindfulness meditation leads to reconfiguration of whole-brain network structure. The reconfiguration of community structure in the brain provides fruitful information about the neural mechanisms of mindfulness meditation.

Author Summary

Training to focus on present-moment experiences, i.e., mindfulness meditation, is known to produce significant beneficial outcomes, such as improved attention and mental health. It is important to understand how these beneficial effects are produced at the neural level; however, previous research investigating this question almost exclusively employed a pre-post design (i.e. assessing brain functioning only once or twice) or comparison between beginners and experts. The current study takes a fundamentally different approach ---- we repeatedly assess the brain function of a single person over many days (intensive longitudinal design) and show that mindfulness mediation significantly changes the size, composition, and variability of the brain networks that are related to sensory processing, executive control, or spontaneous thoughts and self-referential processing. These results highlight the importance of investigating intraindividual changes for understanding the neural mechanisms of mindfulness meditation and suggest that such changes may be used as a biomarker to reflect the efficacy and progress of mindfulness meditation.

Introduction

Mindfulness meditation is a cognitive practice aimed to enhance one's core psychological capacities, such as attentional and emotional self-regulation (1). It involves focused attention to present-moment experiences without emotional reaction and judgment and has been found to produce significant beneficial outcomes, such as stress reduction (2) and improvements in attention processing (3).

Past research indicates that mindfulness meditation is primarily related to three brain networks: the fronto-parietal network (FPN), sensory-motor network (SMN), and default mode network (DMN) (1). The FPN mainly consists of the rostro- and dorso-lateral prefrontal cortex (lPFC), anterior insula, dorsal anterior cingulate cortex (dACC), and anterior inferior parietal lobule (aIPL); all of these brain areas are critical for cognitive control functions, such as regulation of attention and emotion (4–7). Mindfulness meditation, especially in the early stages of long-term practice, increases activation of FPN regions (8–11), which is consistent with the general observation that focusing on the present moment requires effortful attentional control.

Mindfulness meditation also alters sensory experiences through the SMN (12,13), consisting of motor cortices, primary somatosensory cortex, and insula. In a previous study, these brain areas showed reduced activation in a four-day mindfulness meditation when beginners

meditated in the presence of noxious stimulation causing pain (14). This change in brain activity may be associated with enhanced body awareness, as mindfulness meditation requires individuals to focus on a body part or internal experiences, such as breathing (15).

The DMN, mainly consisting of the anterior medial prefrontal cortex (amPFC), posterior cingulate cortex (PCC), and posterior inferior parietal lobule (pIPL), is the network supporting spontaneous thoughts and self-referential processing (16–18). Because mindfulness meditation aims to shut out task-irrelevant thoughts by directing one's attention to an anchoring object such as one's breath, the DMN is expected to be suppressed during mindfulness meditation. In fact, the mPFC and PCC showed less activity during mindfulness meditation, and functional connectivity between the PCC, dACC, and dlPFC was stronger in meditators compared to meditation-naive controls (19). Increased functional connectivity between the PCC and task-positive regions was also observed in a different study (20). These results indicate that mindfulness meditation may increase cognitive control over the DMN functioning (19).

Although the previous work has provided various insights into how mindfulness meditation influences the functional network of the brain, there are two critical limitations in the current literature. First, the brain networks were defined *a priori* in the previous studies, precluding the possibility that mindfulness meditation practice can alter the structure of the primary brain

networks themselves (i.e. FPN, SMN, and DMN). Because recent studies have shown that mindfulness meditation can change functional connectivity across brain regions (10,19,21,22), the whole-brain composition of the FPN, SMN, and DMN may be altered as a consequence of mindfulness meditation.

Second, most of the previous research has employed a one-shot pre-post or nonmeditator-meditator comparison design (23,24), and compared the conditions after aggregating the data across heterogeneous participants. This inter-individual aggregation approach is useful to examine the effects of meditation averaged across participants. However, given the large individual differences in the whole-brain functional connectivity pattern (25,26), there is danger that the approach potentially masks important intra-individual changes in the composition of the brain networks (e.g., some participant-specific network structures may be canceled out by inter-individual aggregation). Therefore, adopting a design that allows us to focus on the intra-individual change may provide novel insights into how mindfulness meditation alters the structure of the brain networks.

The current research aims to expand our understanding of mindfulness meditation by addressing these two critical issues. For that purpose, we will examine the effects of mindfulness meditation using a single-case experimental design with intensive longitudinal data. Single-case experimental designs have a long tradition in psychology (27,28), and in later years, they have been

applied to intensive longitudinal data (for a systematic review, see (29)). Single-case experimental designs are effective in reliably detecting intra-individual changes in outcome variables in response to intervention (29). However, this design has rarely been implemented in neuroimaging studies (for an exception without experimental manipulation, see (30)). Based on this design, we scanned a single participant repeatedly over a long period of time (65 days), employing mindfulness meditation intermittently, and examined whether and how the whole-brain composition of the FPN, SMN, and DMN were altered on the days of mindfulness meditation.

Results

Similarity of the functional connectivity across time

To examine variability of the functional connectivity over time, we calculated correlation of functional connectivity between days (Fig. 1). The correlation value ranged from 0.429 to 0.780, suggesting that the functional connectivity of a single person varies on a daily basis. This result is consistent with previous longitudinal scanning data from a single participant (30).

Finding community structure

To detect the community structure in the time-varying functional connectivity

across the 58 days, we applied a generalized Louvain method (31) (Fig. 2). We defined the dominant community for each ROI for each condition as the community to which the ROI belonged for the largest number of days under the given condition. To label the four communities detected in the current study, we assessed how these communities overlapped with the template communities defined by Yeo et al. (2011)(32). As the result, we labeled the four communities as visual network (80.8% overlap), SMN (50.3% overlap), FPN (45.3% overlap), and DMN (58.4% overlap) (diagonal in Fig. 3A).

Metrics that quantify the changes in community structure

We examined the effect of meditation practice on intra-individual changes in the composition of the whole-brain networks with three metrics: *community size*, *community coherence*, and *flexibility*.

Community size

We defined the community size for a day t as the number of regions included in the time-dependent community on day t. A 2 (practice: MM condition vs. NoMM condition) x 4 (community: Visual network, SMN, FPN, and DMN) mixed-effects analysis of variance of the

number of ROIs within each community showed a significant main effect of community ($F_{(3, 224)}$ = 133.2, $p < 0.001$) while no significant main effect was observed for the condition ($F_{(1, 224)}$ = 0.01, p = 0.911). The interaction between the community and the condition was statistically significant ($F_{(3, 224)}$ = 2.73, p = 0.044), suggesting that there was a significant change in the relative community size between conditions. A simple main effect analysis showed that the FPN community tended to be smaller ($F_{(1, 56)}$ = 2.317, p = 0.134) and the DMN community tended to be larger ($F_{(1, 56)}$ = 2.515, p = 0.118) under the MM compared with NoMM condition.

Fig. 3A shows whether the ROIs stayed in the same community or changed to a different dominant community between the two conditions (i.e. represents the main community that a ROI belonged to under each condition). The on-diagonal brains show the ROIs that stayed in the same dominant community across the two conditions. The off-diagonal brains show the ROIs that belonged to different dominant communities between the two conditions. Consistent with the ANOVA results, the figure shows that a large number of ROIs (i.e. 21 ROIs) that belonged to the FPN in the NoMM condition shifted to the DMN in the MM condition (row 3, column 4; other community pairs ≤ 11 ROIs). The shift in the dominant community affiliation between the conditions is quantitatively depicted in Fig. 3B.

Coherence of community composition

The community size is one way of examining the change in the composition of the brain network across the two conditions. In fact, even if the relative community size is the same between the two conditions, the constituent ROIs of each community may be substantially different in the two conditions. Therefore, for each community, we examined the extent to which the community as identified by the set of ROIs comprising it is stable within each of the two conditions (community coherence). The results of the permutation test are shown in Fig. 4. For the SMN, FPN, and DMN, the coherence of the community structure within the same condition (CONG) was larger than the coherence between the NoMM and MM conditions (INCONG; SMN, $p = 0.030$; FPN, $p = 0.028$; DMN, $p = 0.007$). This result indicates that mindfulness meditation practice has changed the community composition (i.e., the set of ROIs composing the community) in the SMN, FPN, and DMN. The results for the FPN and DMN are a direct consequence of our findings on the community size because a change in the community size implies a decrease in the coherence value. In contrast, the composition of the SMN also changed despite its stable size between the two conditions. For the visual network community, there was no difference in the coherence ($p = 0.137$), which implies that the set of ROIs composing the visual network community was not significantly influenced by mindfulness meditation.

Flexibility of community allegiance

To assess experience-related changes in community allegiance of a ROI, we defined the flexibility of a ROI under each condition using the inverse participation ratio (IPR) (Derrida & Flyvbjerg, 1987). The change in flexibility between MM and NoMM conditions for individual ROIs belonging to each community (i.e. Visual network, SMN, FPN, and DMN) is shown in Fig. 5. Positive values mean that flexibility of the ROI increased as a consequence of mindfulness meditation. One-sample *t*-tests of the difference in flexibility between the two conditions for each community revealed that mindfulness meditation significantly enhanced flexibility of the ROIs in the FPN ($M = 0.17$, $SD = 0.13$, $t = 7.334$, $p < 0.001$). Other communities did not show a significant difference in flexibility of the ROIs ($|M| \leqq 0.02$, $SD \geqq 0.10$, $|t| \leqq 0.802$). These results suggest that mindfulness meditation increases the flexibility of the FPN community, but not the visual network, SMN, or DMN. Table 1 summarizes the results.

Discussion

Previous studies have provided accumulating evidence that mindfulness meditation changes activation and connectivity patterns between specific brain regions (19–21,23,24,33,34).

Extending previous work, we employed a whole-brain graph theoretic analysis with a single-case experimental design using intensive longitudinal data to reveal that mindfulness meditation provokes the reconfiguration of the community structure of the whole-brain functional network.

We found that the size of the FPN decreased and that of the DMN increased as a consequence of mindfulness meditation. This result is consistent with the previously shown enhanced connectivity between the DMN and the FPN (19,20). Brewer and colleagues (2011)(19) reported that experienced meditators showed increased functional connectivity of the PCC with the dACC and dlPFC both during rest and mindfulness meditation. Similarly, Grigg and Grady (2010)(20) reported increased functional connectivity between the PCC and task-positive brain regions. Based on these findings, Brewer et al. (2011)(19) proposed that the composition of these brain networks might have changed over time and become a new "default mode" that can be observed during mindfulness meditation as well as during the resting state (19). The current observation that some ROIs shift from the FPN to the DMN after mindfulness meditation supports their hypothesis.

The FPN, which is one of the critical networks related to mindfulness meditation (1), showed enhanced flexibility under the meditation condition. A previous study suggested that enhanced flexibility in the FPN may reflect an (initial) learning process of a task (35). Accordingly,

although the previous study used a different task with a different time scale, i.e., Bassett et al. (2011)(35) observed the change in the flexibility within a few hours of motor-task training, the increased flexibility in the FPN in the current study may indicate that some form of learning process is operative in mindfulness meditation (e.g., how to control breathing, attention, bodily sensations etc.). Future studies should directly examine whether the enhanced flexibility in the FPN is related to a long-term learning process in mindfulness meditation. If this hypothesis is confirmed, the flexibility of community allegiance in the FPN may be used as a biomarker to assess the efficacy and the progress of mindfulness meditation.

Although the SMN showed a change in coherence across the two conditions, as the FPN and DMN did, the size and flexibility of the SMN were intact. In this sense, mindfulness meditation influenced the SMN but to a lesser extent than it influenced the FPN and DMN. This weaker alteration in the SMN might be because awareness of the body sensation that recruits the SMN (14) is not a primary target of mindfulness meditation in contrast to the attentional enhancement, which is associated with the FPN, and reduction of mind wandering, which is associated with the DMN. One can test this possibility in future research by using an external stimulus (e.g., a fixation) as an object on which attention should be focused during mindfulness meditation rather than a body sensation.

The present study demonstrated the value of a single-case experimental design with

intensive longitudinal data. It allows us to detect intra-individual changes in the whole-brain network composition without being influenced by the large heterogeneity of individuals' brain functional networks (26). Previous studies on mindfulness meditation heavily relied on the expert-beginner and/or pre-post comparison design (1). Future research should be encouraged to adopt the single-case research design more frequently to seek further insights into intra-individual changes in patterns of brain networks as a consequence of mindfulness meditation. One obvious limitation of the current research design is that the data were collected from a single participant, which makes it impossible to examine potential individual differences in our findings. However, although research in cognitive neuroscience typically collects data from multiple participants, for the majority of studies, their main focus is on the aggregated pattern of the brain activation/connectivity (but see person-centered research, e.g., (25)), and individual differences have been typically treated as random noise (sampling error). Therefore, in our view, this limitation is superseded by the strength of the current design: sensitivity to the nuanced intra-individual changes in brain signals and functional connectivity. Nevertheless, the potential of the current intensive longitudinal design would be considerably improved by data obtained from multiple participants in future studies. Another limitation of the present study is that the participant performed mindfulness mediation only for three months, which is considerably shorter than the previous studies with experts (e.g., more than one

year of regular practice) (10). Future research should collect data for a more prolonged period of time to examine how the progress of practice induces long-term changes in the community structure.

Materials and Methods

Ethics Statement

The study was approved by the local institutional review board (UREC 16/28).

Participant

The participant (author S.K.) is a right-handed Asian male, aged 28 years at the onset of the study. The participant is healthy with no history of neuropsychiatric disorders.

The participant underwent 65 scanning sessions, each on a different day between June 15th 2016 and November 11th 2016. The scanning time (between 9am – 5pm) was randomized across days. The data were not acquired on 6 out of the 65 days due to machine troubles and an additional 1 day was excluded due to excessive head movement (> 3.0mm). As a result, data from 58 days were used in the following analyses. On each day, the participant underwent a resting-state fMRI scan with eyes open for 10 minutes and completed two sets of questionnaires carried out for a different study. In 18 out of the 58 days (Fig. 1), the participant underwent a 15-min session of mindfulness

meditation practice a few minutes before scanning. In the practice, the participant tried to focus on his breathing, specifically on sensations of the breath on the nostrils, and attempted to suppress spontaneously upcoming thoughts (10). Before the data collection, the participant studied the mindfulness meditation several times from an auditory instruction developed by a professional trainer (36). In the following text, the "mindfulness meditation (MM) condition" refers to the days on which scanning followed the mindfulness meditation practice. The "no mindfulness meditation (NoMM) condition" refers to the days on which there was no MM practice prior to scanning.

Data acquisition

MR images were acquired using a Siemens 3.0-T Trio scanner equipped with a 32-channel head coil. The resting-state fMRI data were obtained using a single-shot, gradient-echo echo-planar imaging (EPI) sequence. Sequence parameters were as follows: repetition time/echo time (TR/TE) = 2,500/30 ms, slice thickness = 3.5 mm, field of view (FoV) = 256 mm, flip angle (FA) = 90°, data matrix = 64 × 64, in-plane resolution = 3.5 × 3.5 mm, 46 slices, 10 minutes scan length. Four dummy scans were discarded to remove the impact of magnetization instability. A high-resolution (spatial resolution: 1 × 1 × 1 mm) structural image was also acquired on the first day using a T1-weighted magnetization prepared rapid-acquisition gradient echo (MP-RAGE) pulse sequence.

Data preprocessing

All preprocessing steps were performed using the Data Processing Assistant for Resting-State fMRI Advanced Edition (DPARSFA) (37), which runs on Statistical Parametric Mapping 8 (SPM8) and the Resting-State fMRI Data Analysis Toolkit (REST) (38). Data preprocessing included the following steps: realignment of all functional images using a six-parameter rigid body transformation; slice-timing correction to the middle slice of each volume; co-registration of the structural image (T1-weighted MPRAGE) to the mean functional image using a rigid-body transformation; segmentation of the transformed structural image into the gray matter, white matter, and cerebrospinal fluid (CSF); nuisance covariate regression of six head motion parameters, average white matter signals, CSF signals, and the global signal in native space; spatial normalization of the functional images to the Montreal Neurological Institute (MNI) stereotactic standard space; spatial smoothing of the functional images with a 6-mm full-width at half-maximum (FWHM) Gaussian kernel using the Diffeomorphic Anatomical Registration Through Exponentiated Lie Algebra (DARTEL) toolbox (39); band-pass filtering (0.01–0.10 Hz) to reduce low-frequency drift and high-frequency physiological noise.

Computation of functional connectivity

To calculate a functional connectivity matrix for each day, we defined the regions of interest (ROI) based on the Human Connectome Project (HCP)'s multi-modal parcellation version 1.0 (40) and the automated anatomical labeling (AAL) atlas (41). Of the 360 cerebral cortical ROIs defined by the HCP, one ROI (rh.R_8BL) was excluded because the obtained mask contained only 2 voxels. In addition to the remaining 359 cerebral cortical ROIs, we included 40 limbic and cerebellar ROIs defined by AAL, resulting in a total of 399 ROIs. For each ROI, we computed the spatial average of the signal within the mask. For each day, we quantified functional connectivity between each pair of the 399 ROIs by the absolute value of the Pearson correlation coefficient between the two fMRI time-course signals (42,43).

Similarity of the functional connectivity across time

To calculate correlation of functional connectivity between days. Specifically, we first vectorized the functional connectivity between all pairs of 399 ROIs for each day into a $399 \times 398 / 2 = 79{,}401$ dimensional vector. Then, we computed the Pearson's correlation coefficient between the two vectors for the corresponding days.

Generalized Louvain method

The original Louvain method approximately maximizes the objective function (modularity) to partition the nodes in the given static network into communities. Communities are determined such that there are many edges within each community and relatively few edges between communities (44). The generalized Louvain method considers the edges across multiple inter-dependent slices and optimizes the generalized modularity instead of separately optimizing the modularity for each slice. In the present study, a slice represents the static functional connectivity on one day. We ran the algorithm 100 times and selected the community structure yielding the largest generalized modularity value. As shown in the Results section, this procedure found four communities.

Community labeling

First, we represented each community i (i = 1, 2, 3, 4) by its core members. The core members of the ith community were defined by the ROIs whose dominant community was the ith community under both conditions. The relative overlap between the ith community and a community in the template, N_j (j = 1, 2, ..., 7), was defined as $V_{(C_i \cap N_j)} / \sum_{l=1}^{7} V_{(C_i \cap N_j)}$, where C_i is the set of voxels belonging to a core member of the ith community, N_j is interpreted as the set of voxels

belonging to mask N_j, and $V_{(C_i \cap N_j)}$ represents the number of voxels that belong to both C_i and N_j. We then labeled each community *i* according to the community in the template that exhibited the largest overlap with the *i*th community.

Calculation and statistical significance test of community coherence

We defined the similarity of each community *i* (*i* = 1, 2, 3, 4) between day t_1 and day t_2 by the Jaccard index, i.e. $J_{(X,Y)} = |X \cap Y|/|X \cup Y|$, where *X* is the set of nodes in community *i* on day t_1 and *Y* is the set of nodes in community *i* on day t_2. Jaccard index $J_{(X,Y)}$ ranges between 0 and 1. One obtains $J_{(X,Y)} = 1$ if and only if *X* and *Y* are exactly the same, and $J_{(X,Y)} = 0$ if *X* and *Y* do not share any ROIs. For each of the four communities, we calculated the similarity between all pairs of 58 days, obtaining a 58 $\times$ 58 similarity matrix.

Given the similarity matrix for a community, we compared the coherence of the community within and across the practice conditions. Specifically, we adapted a permutation test, which is commonly used for testing the significance of single-subject research (45). The permutation test consists of the following three steps. In the first step, we classified the pairs of days into two groups. The congruent (CONG) group contained the pairs of days which both belonged to the MM condition or the pair of days which both belonged to the NoMM condition. In contrast, the

incongruent (INCONG) group contained the pairs of days from the different conditions (i.e. one from the MM condition and the other from the NoMM condition). Because there were 18 MM days and 40 NoMM days, CONG and INCONG groups contained 933 and 720 pairs of days, respectively. In the second step, we computed the coherence of the community, which is a Welch's *t*-value, by comparing the averaged similarity value between the CONG and INCONG groups. We then randomized the days by reassigning 18 uniformly randomly selected days to the fictive MM condition and the remaining 40 days to the fictive NoMM condition, and calculated the coherence for the randomized data. We repeated this procedure 10,000 times to obtain the null distribution of the coherence for the randomized labeling. In the third step, we assessed the probability of obtaining the coherence calculated on the basis of the true labeling of the days (i.e., MM or NoMM) or more extreme coherence under the null model in which the MM condition was randomly assigned to individual days.

Calculation and statistical significance test of flexibility

We defined the flexibility of a ROI under each condition using the inverse participation ratio (IPR) (46). The IPR of a ROI under a condition is defined as

$$IPR = 1 - \sum_{i=1}^{4} \left(\frac{I_i}{I}\right)^2,$$

where I represents the number of days (NoMM condition, 40; MM condition, 18), and I_i represents the number of days in which the ROI belonged to community i (i = 1, 2, 3, 4). The IPR is equal to 0.75, which is the largest possible value, when a ROI belongs to all the communities with the same probability. In this case, the ROI is the most flexible in terms of the community membership. The IPR is equal to 0, which is the smallest possible value, when the ROI belongs to the same single community in all the days. In this case, the ROI is the least flexible. To investigate whether the mindfulness meditation affects the community-wide flexibility of ROIs, for each community, we applied a paired sample t-test to test the mean difference in the flexibility between the two conditions. In this particular analysis, we defined each community i by its core members, i.e., the ROIs that belonged to community i as the dominant community under both conditions.

Acknowledgements

This research was supported by the Marie Curie Career Integration Grant, Award Number CIG630680; JSPS KAKENHI (Grant Numbers 15H05401; 16H06406, 18H01102; 18K18696), F. J. McGuigan Early Career Investigator Prize from American Psychological Foundation; and the Leverhulme Trust (Grant Numbers RPG-2016-146 and RL-2016-030).

References

1. Tang Y-Y, Hölzel BK, Posner MI. The neuroscience of mindfulness meditation. Nat Rev Neurosci [Internet]. 2015;16(4):1–13. Available from: http://dx.doi.org/10.1038/nrn3916%5Cnpapers3://publication/doi/10.1038/nrn3916
2. Goldin PR, Gross JJ. Effects of Mindfulness-Based Stress Reduction (MBSR) on Emotion Regulation in Social Anxiety Disorder. Emotion. 2010;10(1):83–91.
3. van den Hurk PAM, Giommi F, Gielen SC, Speckens AEM, Barendregt HP. Greater efficiency in attentional processing related to mindfulness meditation. Q J Exp Psychol. 2010;63(6):1168–80.
4. Dosenbach NUF, Fair D a, Cohen AL, Schlaggar BL, Petersen SE. A dual-networks architecture of top-down control. Trends Cogn Sci [Internet]. 2008 Mar [cited 2014 May 8];12(3):99–105. Available from: http://www.pubmedcentral.nih.gov/articlerender.fcgi?artid=3632449&tool=pmcentrez&rendertype=abstract
5. Spreng RN, Stevens WD, Chamberlain JP, Gilmore AW, Schacter DL. Default network activity, coupled with the frontoparietal control network, supports goal-directed cognition. Neuroimage [Internet]. 2010 Oct 15 [cited 2012 Jul 14];53(1):303–17. Available from:

http://www.pubmedcentral.nih.gov/articlerender.fcgi?artid=2914129&tool=pmcentrez&rendertype=abstract

6. Sridharan D, Levitin DJ, Menon V. A critical role for the right fronto-insular cortex in switching between central-executive and default-mode networks. Proc Natl Acad Sci U S A [Internet]. 2008 Aug 26;105(34):12569–74. Available from: http://www.pubmedcentral.nih.gov/articlerender.fcgi?artid=2527952&tool=pmcentrez&rendertype=abstract

7. Vincent JL, Kahn I, Snyder AZ, Raichle ME, Buckner RL. Evidence for a Frontoparietal Control System Revealed by Intrinsic Functional Connectivity. J Neurophysiol [Internet]. 2008;100(6):3328–42. Available from: http://jn.physiology.org/cgi/doi/10.1152/jn.90355.2008

8. Brefczynski-Lewis JA, Lutz A, Schaefer HS, Levinson DB, Davidson RJ. Neural correlates of attentional expertise in long-term meditation practitioners. Proc Natl Acad Sci [Internet]. 2007;104(27):11483–8. Available from: http://www.pnas.org/cgi/doi/10.1073/pnas.0606552104

9. Chiesa a, Serretti a. A systematic review of neurobiological and clinical features of mindfulness meditations. Psychol Med [Internet]. 2010 Aug [cited 2014 Apr 28];40(8):1239–52. Available from: http://www.ncbi.nlm.nih.gov/pubmed/19941676

10. Hasenkamp W, Wilson-Mendenhall CD, Duncan E, Barsalou LW. Mind wandering and attention during focused meditation: A fine-grained temporal analysis of fluctuating cognitive states. Neuroimage [Internet]. 2012;59(1):750–60. Available from: http://dx.doi.org/10.1016/j.neuroimage.2011.07.008

11. Malinowski P. Neural mechanisms of attentional control in mindfulness meditation. Front Neurosci. 2013;7(7 FEB):1–11.

12. Berkovich-Ohana A, Glicksohn J, Goldstein A. Mindfulness-induced changes in gamma band activity - Implications for the default mode network, self-reference and attention. Clin Neurophysiol [Internet]. 2012;123(4):700–10. Available from: http://dx.doi.org/10.1016/j.clinph.2011.07.048

13. Cahn BR, Delorme A, Polich J. Occipital gamma activation during Vipassana meditation. Cogn Process. 2010;11(1):39–56.

14. Zeidan F, Martucci KT, Kraft RA, Gordon NS, McHaffie JG, Coghill RC. Brain Mechanisms Supporting the Modulation of Pain by Mindfulness Meditation. J Neurosci [Internet]. 2011;31(14):5540–8. Available from: http://www.jneurosci.org/cgi/doi/10.1523/JNEUROSCI.5791-10.2011

15. Kabat-Zinn J. Mindfulness Meditation for Everyday Life [Internet]. 2009. 279 p. Available

from:
http://search.chadpearce.com/Home/BOOKS/97291641-Mindfulness-Meditation-for-Everyday-Life-Kabat-Zinn-Jon.pdf

16. Christoff K, Irving ZC, Fox KCR, Spreng RN, Andrews-Hanna JR. Mind-wandering as spontaneous thought: a dynamic framework. Nat Rev Neurosci [Internet]. 2016;17:718–31. Available from: http://dx.doi.org/10.1038/nrn.2016.113

17. Kajimura S, Kochiyama T, Abe N, Nomura M. Challenge to Unity : Relationship Between Hemispheric Asymmetry of the Default Mode Network and Mind Wandering. 2018;(April):1–11.

18. Smallwood J, Schooler JW. The Science of Mind Wandering: Empirically Navigating the Stream of Consciousness. Annu Rev Psychol [Internet]. 2015;66(1):487–518. Available from: http://www.annualreviews.org/doi/10.1146/annurev-psych-010814-015331

19. Brewer J a, Worhunsky PD, Gray JR, Tang Y-Y, Weber J, Kober H. Meditation experience is associated with differences in default mode network activity and connectivity. Proc Natl Acad Sci U S A [Internet]. 2011 Dec 13 [cited 2014 May 1];108(50):20254–9. Available from: http://www.pubmedcentral.nih.gov/articlerender.fcgi?artid=3250176&tool=pmcentrez&rendertype=abstract

20. Grigg O, Grady CL. Task-related effects on the temporal and spatial dynamics of resting-state functional connectivity in the default network. PLoS One. 2010;5(10):1–12.

21. Kilpatrick L a, Suyenobu BY, Smith SR, Bueller J a, Goodman T, Creswell JD, et al. Impact of Mindfulness-Based Stress Reduction training on intrinsic brain connectivity. Neuroimage [Internet]. 2011 May 1 [cited 2014 May 1];56(1):290–8. Available from: http://www.pubmedcentral.nih.gov/articlerender.fcgi?artid=3072791&tool=pmcentrez&rendertype=abstract

22. Taylor VA, Daneault V, Grant J, Scavone G, Breton E, Roffe-vidal S, et al. Impact of meditation training on the default mode network during a restful state. Soc Cogn Affect Neurosci. 2013;8(1):4–14.

23. Tang YY, Posner MI. Attention training and attention state training. Trends Cogn Sci. 2009;13(5):222–7.

24. Zeidan F, Martucci KT, Kraft R a, McHaffie JG, Coghill RC. Neural correlates of mindfulness meditation-related anxiety relief. Soc Cogn Affect Neurosci [Internet]. 2013 Jun 3 [cited 2014 Jun 1]; Available from: http://www.ncbi.nlm.nih.gov/pubmed/23615765

25. Bansal K, Nakuci J, Muldoon SF. Personalized brain network models for assessing structure–function relationships. Curr Opin Neurobiol [Internet]. 2018;52:42–7. Available from:

https://doi.org/10.1016/j.conb.2018.04.014

26. Mueller S, Wang D, Fox MD, Yeo BTT, Sepulcre J, Sabuncu MR, et al. Individual Variability in Functional Connectivity Architecture of the Human Brain. Neuron [Internet]. 2013;77(3):586–95. Available from: http://dx.doi.org/10.1016/j.neuron.2012.12.028

27. Fechner GT. Elemente der psychophysik [Elements of psychophysics]. Leipzig, Germany: Breitkopf & Hartel; 1889.

28. Watson JB. Behaviorism. New York, NY: Norton; 1925.

29. Smith JD. Single-Case Experimental Designs: A Systematic Review of Published Research and Current Standards. Pychological Methods. 2013;17(4):1–70.

30. Poldrack RA, Laumann TO, Koyejo O, Gregory B, Hover A, Chen M-Y, et al. Long-term neural and physiological phenotyping of a single human. Nat Commun [Internet]. 2015;6:8885. Available from: http://www.nature.com/ncomms/2015/151209/ncomms9885/full/ncomms9885.html

31. Jeub LGS, Bazzi M, Jutla IS, Mucha PJ. A generalized Louvain method for community detection implemented in MATLAB. 2017.

32. Yeo BTT, Krienen FM, Sepulcre J, Sabuncu MR, Lashkari D, Hollinshead M, et al. The organization of the human cerebral cortex estimated by intrinsic functional connectivity. J

Neurophysiol [Internet]. 2011;106:1125–65. Available from: http://jn.physiology.org/content/106/3/1125.short

33. Hasenkamp W, Barsalou LW. Effects of Meditation Experience on Functional Connectivity of Distributed Brain Networks. Front Hum Neurosci [Internet]. 2012;6(March):1–14. Available from: http://journal.frontiersin.org/article/10.3389/fnhum.2012.00038/abstract

34. Taylor VA, Daneault V, Grant J, Scavone G, Breton E, Roffe-Vidal S, et al. Impact of meditation training on the default mode network during a restful state. Soc Cogn Affect Neurosci [Internet]. 2013 Mar 24 [cited 2012 Jul 18];8(1):4–14. Available from: http://scan.oxfordjournals.org/content/early/2012/03/24/scan.nsr087.short

35. Bassett DS, Wymbs NF, Porter MA, Mucha PJ, Carlson JM, Grafton ST. Dynamic reconfiguration of human brain networks during learning. Proc Natl Acad Sci USA [Internet]. 2011;108(18):7641–6. Available from: http://arxiv.org/abs/1010.3775%0Ahttp://dx.doi.org/10.1073/pnas.1018985108

36. Fujino M, Ueda Y, Inoue V, Shigematsu SM, Sanders JG. Development of brief single-session instructions of focused attention, open monitoring, and compassion meditation for psychological experiment.

37. Chao-Gan Y, Yu-Feng Z. DPARSF: a MATLAB toolbox for “pipeline” data analysis of

resting-state fMRI. Front Syst Neurosci [Internet]. 2010;4(13):1–7. Available from: http://journal.frontiersin.org/article/10.3389/fnsys.2010.00013/abstract

38. Song XW, Dong ZY, Long XY, Li SF, Zuo XN, Zhu CZ, et al. REST: A Toolkit for resting-state functional magnetic resonance imaging data processing. PLoS One. 2011;6(9).

39. Ashburner J. A fast diffeomorphic image registration algorithm. Neuroimage. 2007;38(1):95–113.

40. Glasser MF, Coalson TS, Robinson EC, Hacker CD, Harwell J, Yacoub E, et al. A multi-modal parcellation of human cerebral cortex. Nature [Internet]. 2016;536(7615):171–8. Available from: http://www.ncbi.nlm.nih.gov/pubmed/27437579%5Cnhttp://www.pubmedcentral.nih.gov/articlerender.fcgi?artid=PMC4990127

41. Tzourio-Mazoyer N, Landeau B, Papathanassiou D, Crivello F, Etard O, Delcroix N, et al. Automated anatomical labeling of activations in SPM using a macroscopic anatomical parcellation of the MNI MRI single-subject brain. Neuroimage [Internet]. 2002 Jan [cited 2014 Apr 28];15(1):273–89. Available from: http://www.ncbi.nlm.nih.gov/pubmed/11771995

42. Achard S. A Resilient, Low-Frequency, Small-World Human Brain Functional Network with Highly Connected Association Cortical Hubs. J Neurosci [Internet]. 2006;26(1):63–72.

Available from: http://www.jneurosci.org/cgi/doi/10.1523/JNEUROSCI.3874-05.2006

43. Fallani FDV, Richiardi J, Chavez M, Achard S. Graph analysis of functional brain networks: practical issues in translational neuroscience. 2014;(September). Available from: http://arxiv.org/abs/1406.7391

44. Blondel VD, Guillaume J-L, Lambiotte R, Lefebvre E. Fast unfolding of communities in large networks. J Stat Mech Theory Exp [Internet]. 2008;10008(10):6. Available from: http://arxiv.org/abs/0803.0476

45. Edgington ES. Validity of randomization tests for one-subject experiments. J Educ Stat. 1980;5(3):235–51.

46. Derrida, B; Flyvbjerg H. Multivalley Structures in Disordered Systems. 1987;20:5273–88.

Figure legends and Tables

Figure 1. Similarity (correlation) between the functional networks for each pair of days. The color code represents the value of the correlation coefficient.

Figure 2. Time-dependent community structure. The rows and columns correspond to the days and ROIs, respectively. The meditation days are colored in black in the rightmost column. The four communities were labeled the visual network (colored in purple), sensory-motor network (SMN; green), fronto-parietal network (FPN; blue), and default mode network (DMN; red). A white stripe describes a day in which a ROI belonged to more than one community and could not be assigned a community label.

Figure 3. The change of dominant community affiliation between the NoMM and MM conditions. (A) The shift of the dominant community allegiance of ROIs between the conditions. The schematic pictures of the brain on the diagonal show the ROIs that belonged to the same community with the highest probability across the two conditions. Those off the diagonal show the ROIs that belonged to different communities in the two conditions. (B) Quantitative description of dominant community shift across the conditions.

Figure 4. Coherence of the community within and across conditions. Coherence is a Welch's *t*-value that represents the difference in averaged similarity value of a community structure between two groups, i.e., the congruent (CONG) and incongruent (INCONG) group. The CONG group contained pairs of days that both belonged to the MM condition or the NoMM condition. The INCONG group contained the pairs of days from the different conditions (i.e. one from the MM condition and the other from the NoMM condition). The figure shows null distributions of coherence (distributions of coherence for permutated data); vertical lines represent the *t*-values observed with the true labeling and their corresponding *p*-values representing the probability of obtaining such observed *t*-values (or more extreme *t*-values) in the null distribution.

Figure 5. Changes in flexibility of ROIs between two conditions. Histograms for each community show the distribution of the values of ROIs that belonged to the corresponding community in both conditions.

Table 1. Summary of the meditation effect. *n.s.* indicates not significant.

Network	Size The number of ROIs in the community	Coherence Change in the composition of ROIs in a community	Flexibility Frequency with which ROIs change their community allegiance
Visual	*n.s.*	*n.s.*	*n.s.*
SMN	*n.s.*	NoMM ≠ MM	*n.s.*
FPN	NoMM > MM	NoMM ≠ MM	NoMM < MM
DMN	NoMM < MM	NoMM ≠ MM	*n.s.*

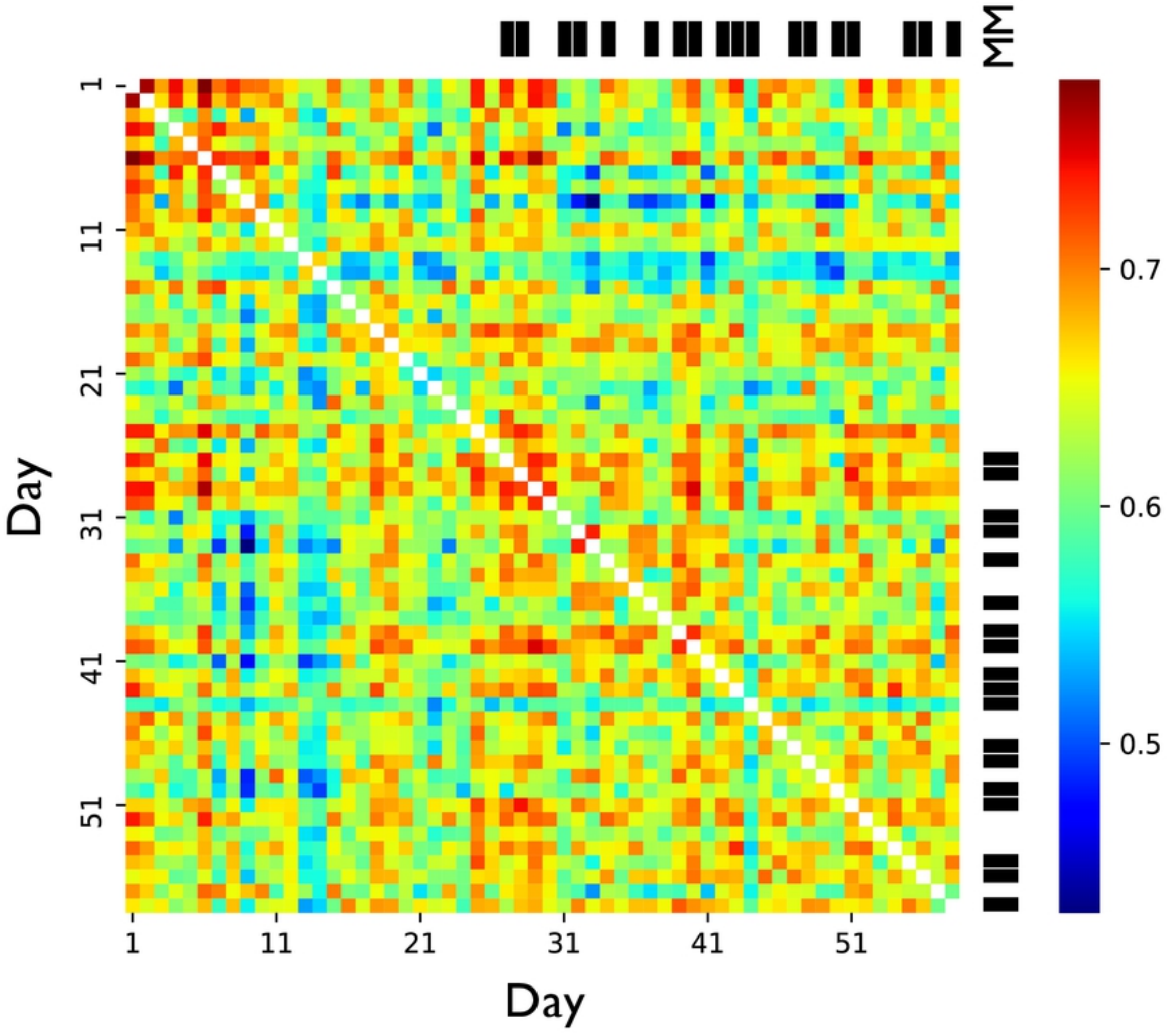
MM
1
11
21
31
41
51
Day
1
11
21
31
41
51
Day
0.7
0.6
0.5

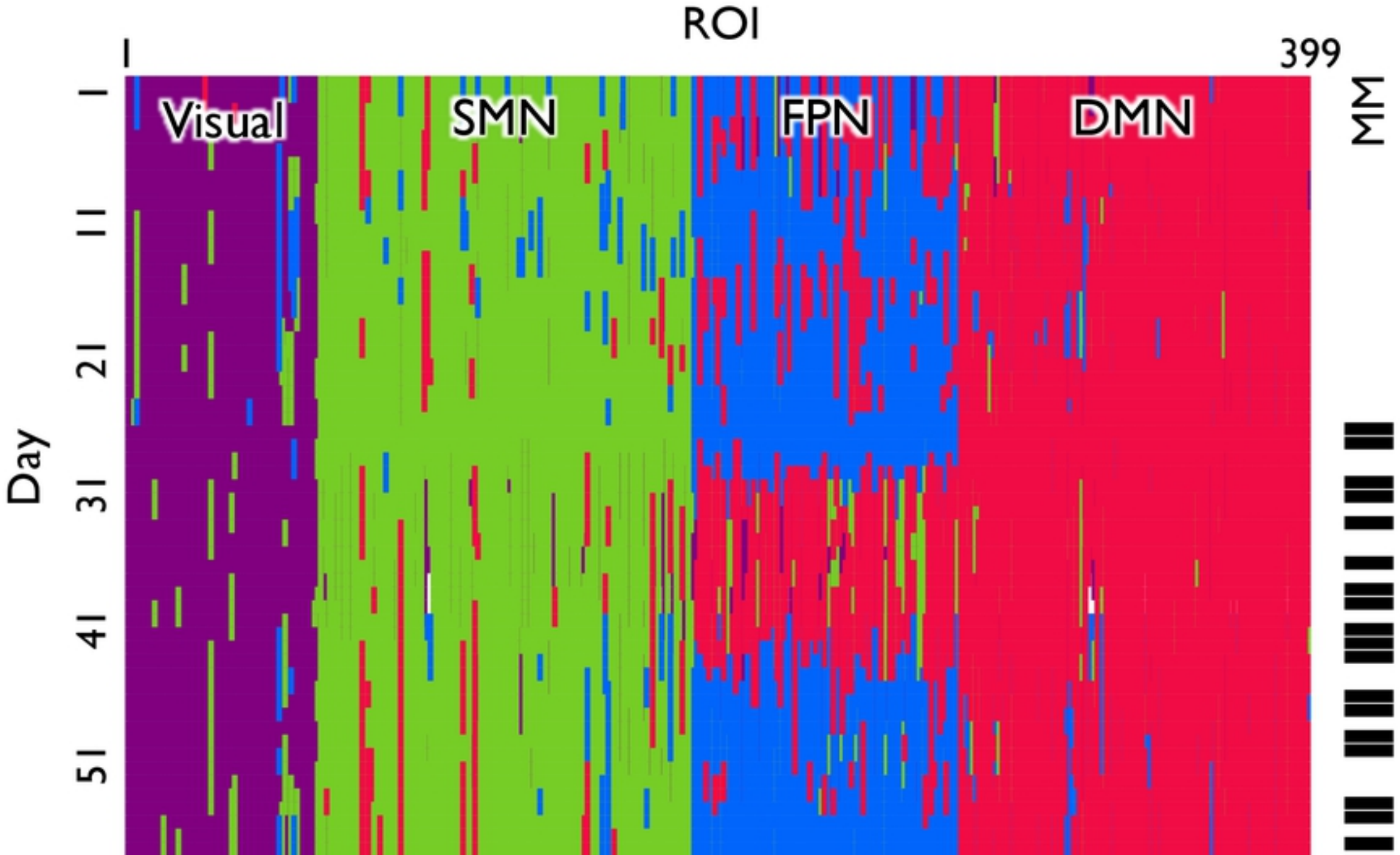
ROI
1
399
Visual
SMN
FPN
DMN
MM
Day
1
11
21
31
41
51

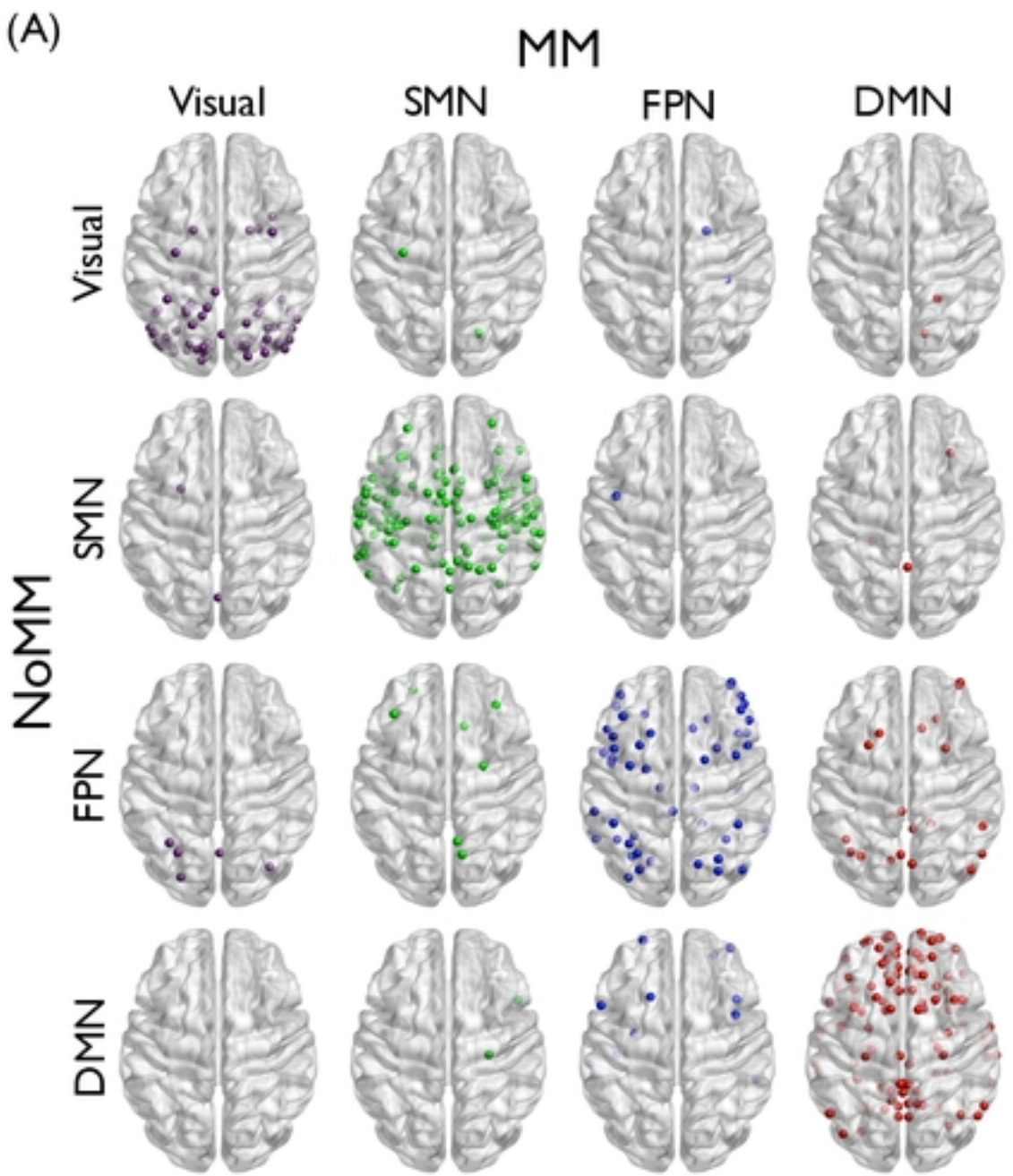
(A)
MM
Visual
SMN
FPN
DMN
NoMM
Visual
SMN
FPN
DMN

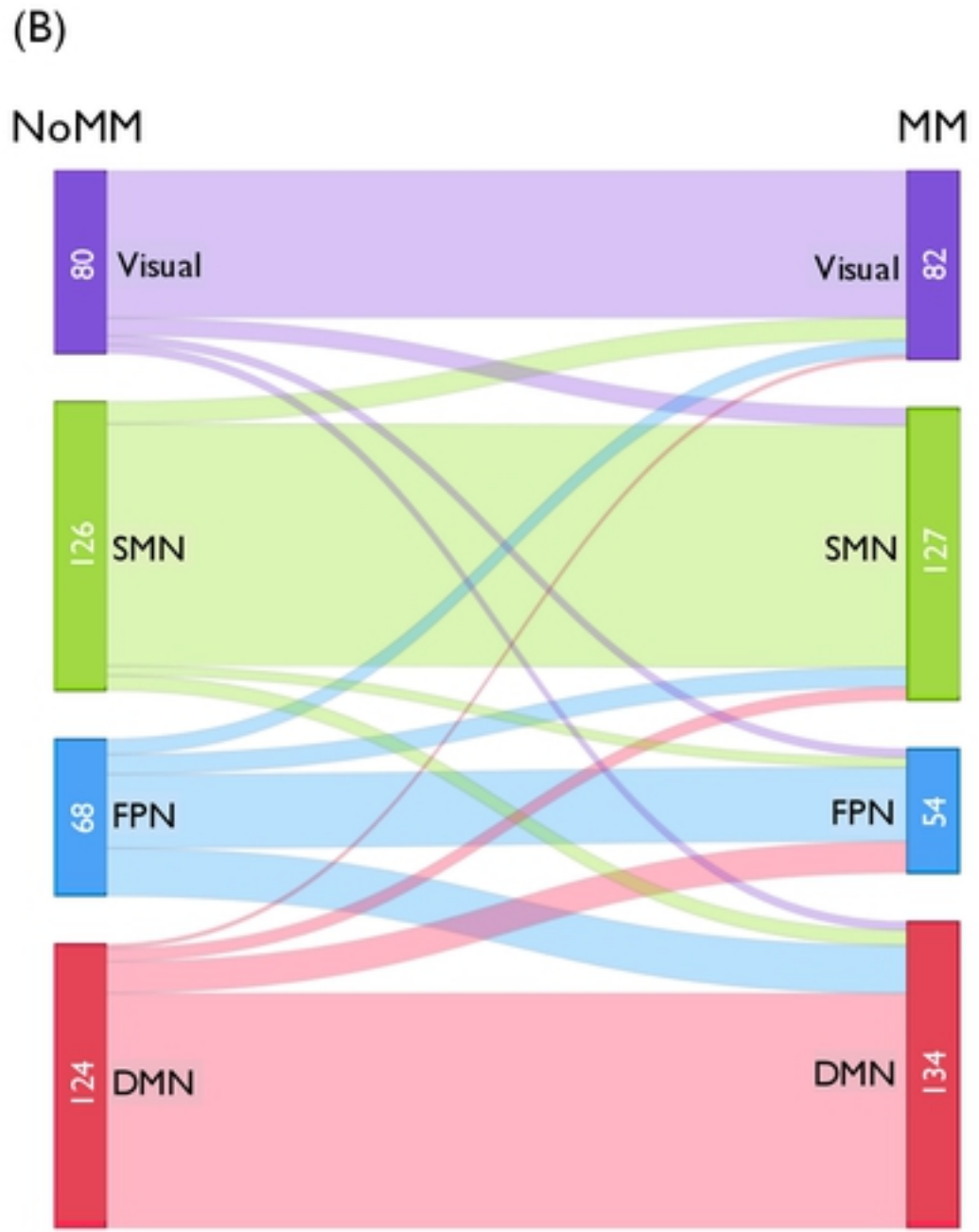
(B)
NoMM
MM
80
Visual
126
SMN
68
FPN
124
DMN
Visual
82
SMN
127
FPN
54
DMN
134

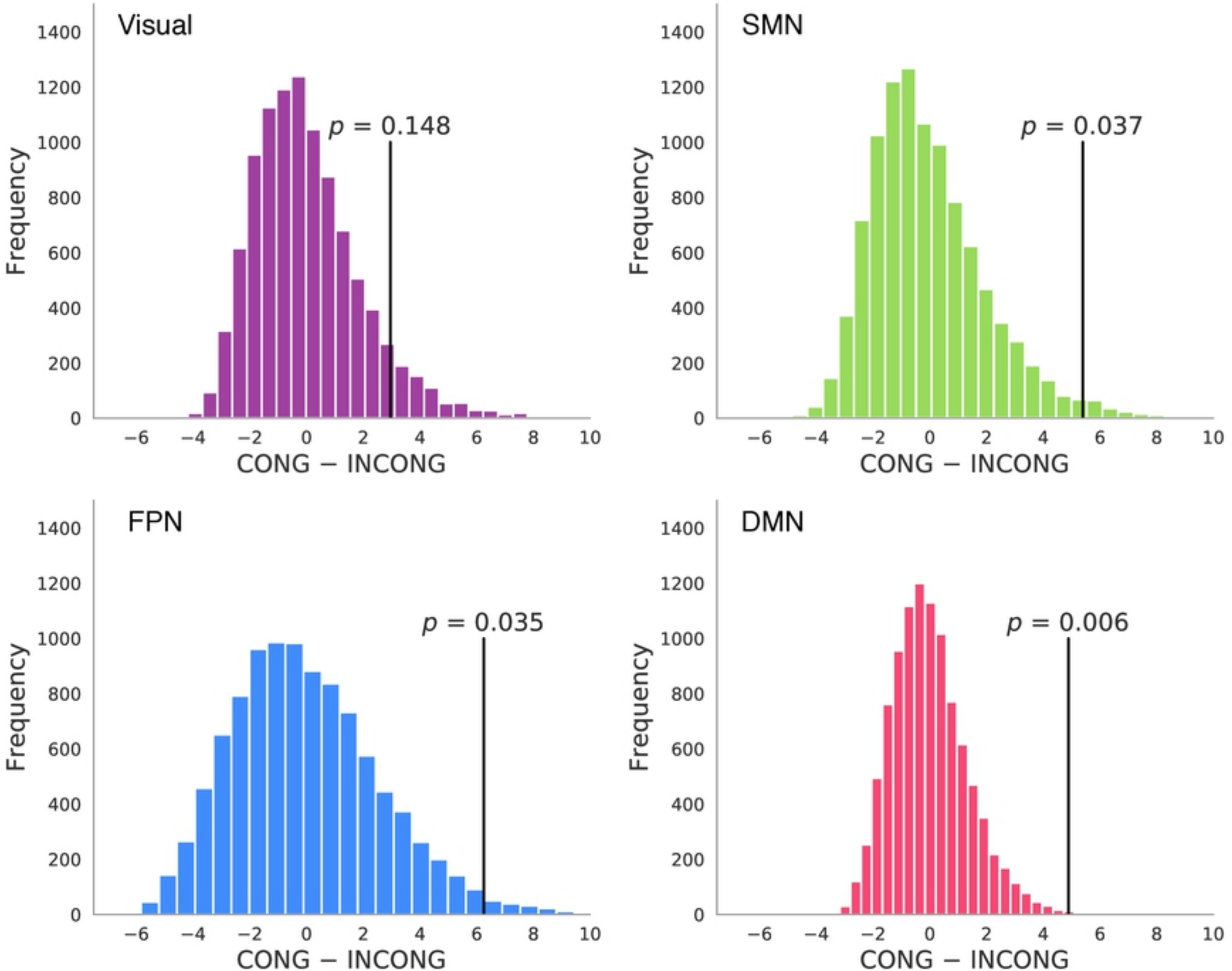
Visual
p = 0.148
SMN
p = 0.037
FPN
p = 0.035
DMN
p = 0.006
Frequency
CONG − INCONG
0
200
400
600
800
1000
1200
1400
−6
−4
−2
0
2
4
6
8
10

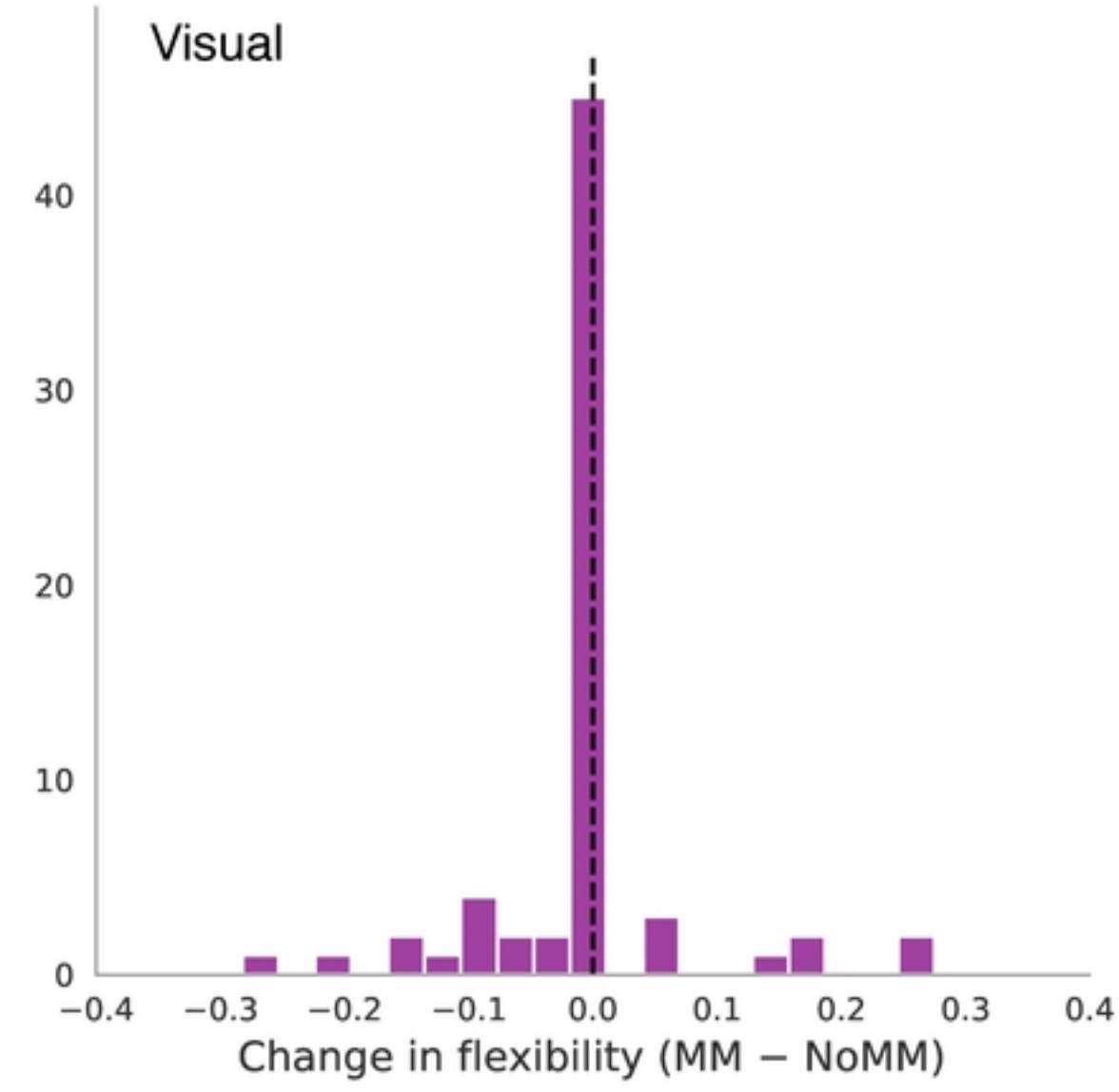
Visual
0
10
20
30
40
−0.4
−0.3
−0.2
−0.1
0.0
0.1
0.2
0.3
0.4
Change in flexibility (MM − NoMM)

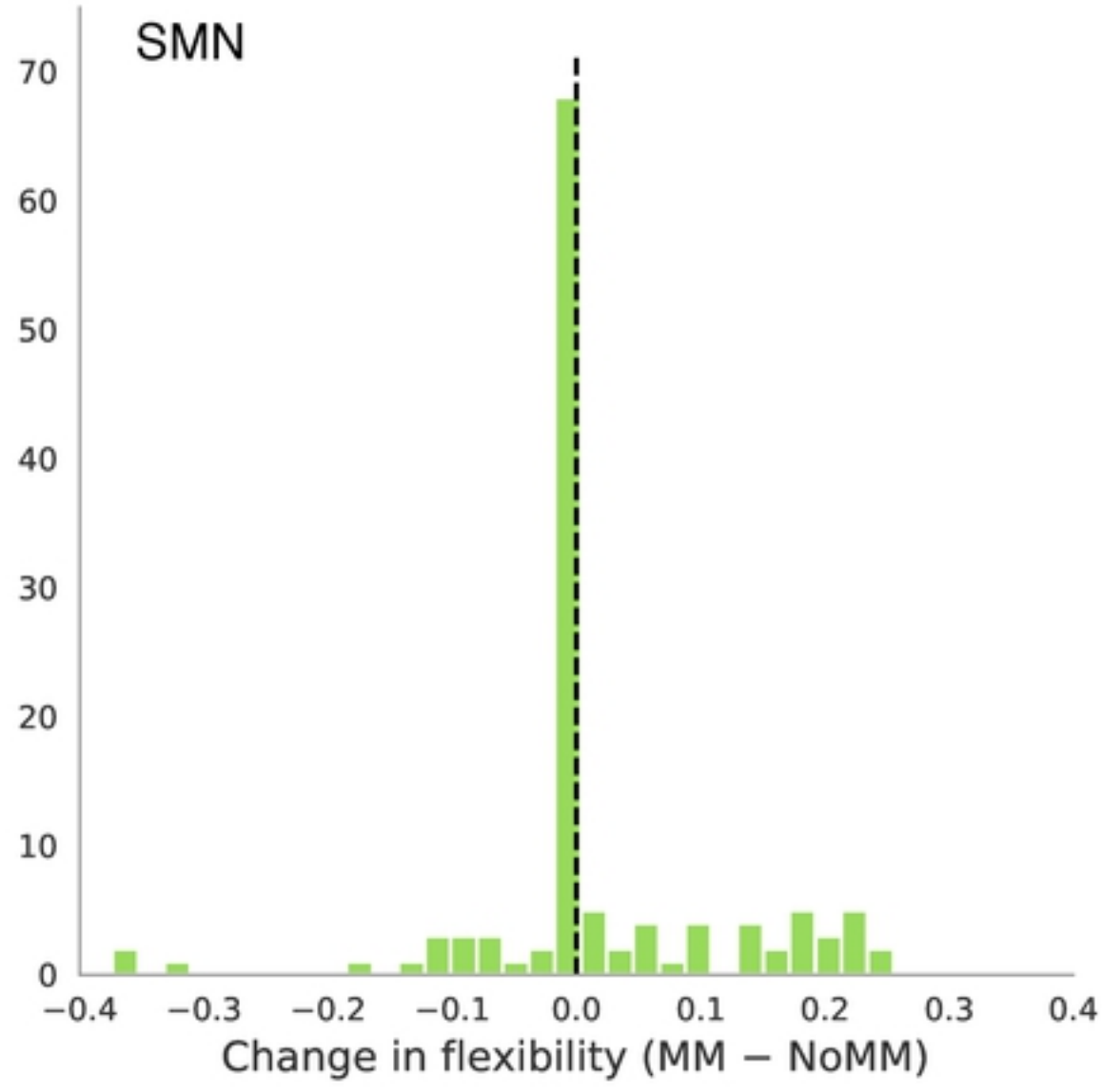
SMN
0
10
20
30
40
50
60
70
−0.4
−0.3
−0.2
−0.1
0.0
0.1
0.2
0.3
0.4
Change in flexibility (MM − NoMM)

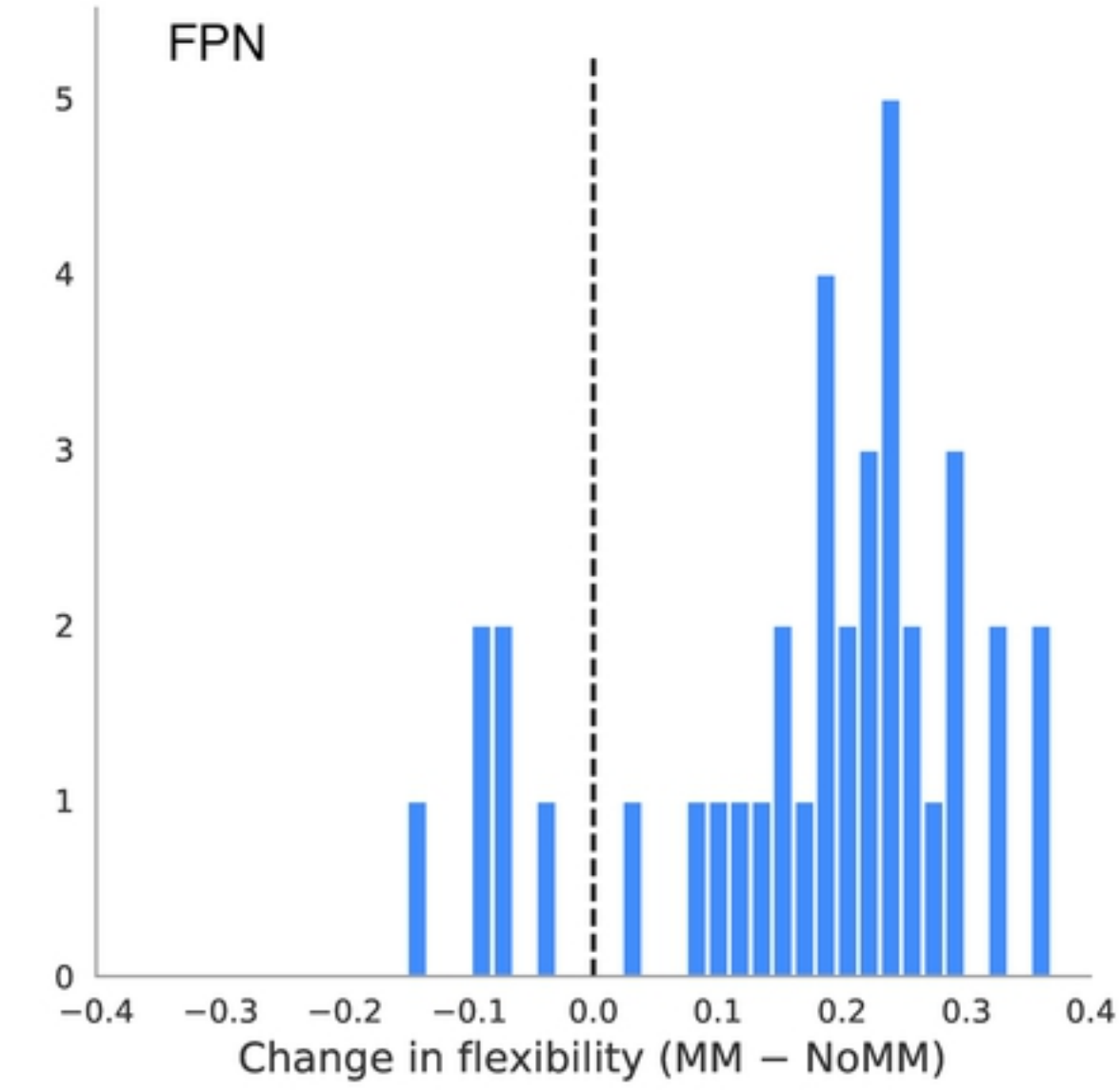
FPN
0
1
2
3
4
5
−0.4
−0.3
−0.2
−0.1
0.0
0.1
0.2
0.3
0.4
Change in flexibility (MM − NoMM)

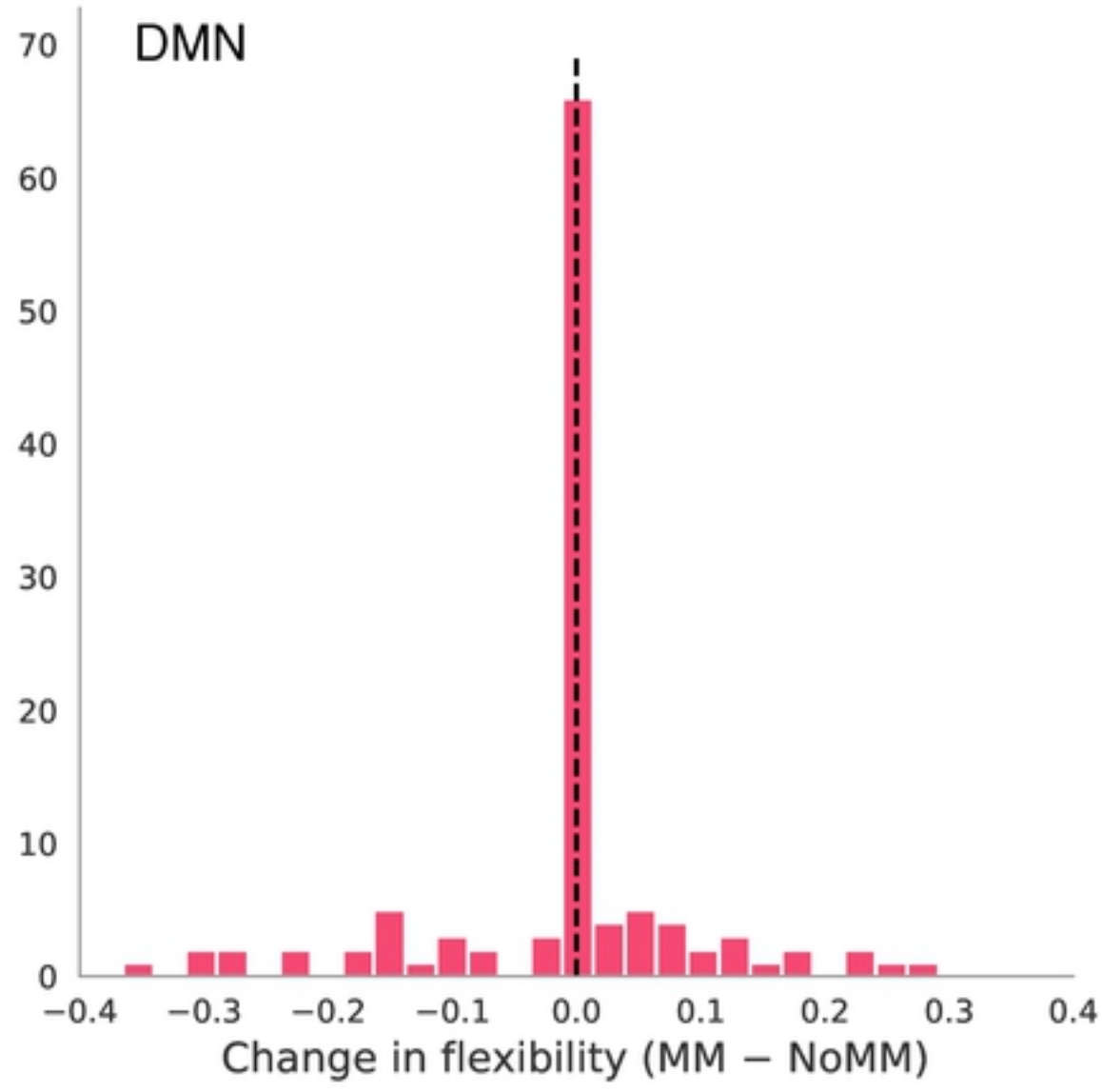
DMN
0
10
20
30
40
50
60
70
−0.4
−0.3
−0.2
−0.1
0.0
0.1
0.2
0.3
0.4
Change in flexibility (MM − NoMM)